

Load spectrum estimation from output-only measurements applied to a spray boom model

K. Engelen, H. Ramon, J. Anthonis

K.U.Leuven, MeBioS,

Kasteelpark Arenberg 30, B-3001, Heverlee, Belgium

e-mail: kurt.engelen@biw.kuleuven.be

Abstract

A finite element model is constructed representing the dynamic behavior of a spray boom. The model is updated with experimental vibration data obtained from field measurements. The spectra of the input forces are identified from these measurements and based on a parameterized spectrum model, a classification is made between normal and rough spraying conditions.

1 Introduction

Spray booms are used to distribute pesticides and liquid fertilizer over the fields. The common practice is to cover the field as homogeneously as possible. Extensive studies based on field experiments, mathematical models and simulations pointed out that spray boom motions have a dramatic effect on the spray distribution pattern. Since spray boom widths are continuously increasing, reaching values up to 50m nowadays, this problem has become a very critical issue. Besides the non-uniformity of the spray pattern, also severe strength problems arise for the large booms.

To reduce these motions, the eigenmodes of the spray boom should be damped. This can be done by placing dampers on the structure. Therefore it has to be investigated which are the most important eigenmodes that affect the spray pattern. A good damper location and the optimal damper characteristic resulting in minimized vibrations have to be found. Besides, dampers with different characteristics have to be compared. This is investigated by time domain analysis, because non-linear elements are treated. Moreover, the calculation of the spray pattern requires time histories of the boom movements. This means that besides from a model describing the dynamic behavior of a spray boom, also dynamic loads are required for such simulations.

To obtain such model and loads, there are many different possibilities. If the system consisting of tractor, trailer and spray boom (figure 1) is modeled as a whole, standard road surface profiles can be used as input loads to the six tires. It is commonly known that vertical accelerations of road vehicles are ultimately caused by road roughness [1]. Nevertheless, there is little information found in literature about the relation between horizontal vehicle vibrations and vertical inputs from road roughness. In this case, we are mainly interested in the horizontal vibrations of the spray boom, because non-uniformity of the spray distribution is mainly caused by horizontal boom vibrations [2]. Moreover, in the case of off-road vehicles, the influence of soil deformation should be taken into account, which complicates the problem. Therefore, this possibility is rejected.

A second opportunity, which will be applied here, is to estimate the input loads from acceleration data obtained by field measurements, using an inverse method. In order for this method to be able to be successful, the mathematical model and the real system should match very well. This can be achieved by updating the parameters of the model by the experimental vibration data.

The problem of model updating is a research topic that has been widely investigated in the area of structural dynamics [3]. For civil structures, the common approach is to use modal parameters such as eigenfrequen-



Figure 1: Picture of the tractor-trailer-sprayboom combination on the shaker

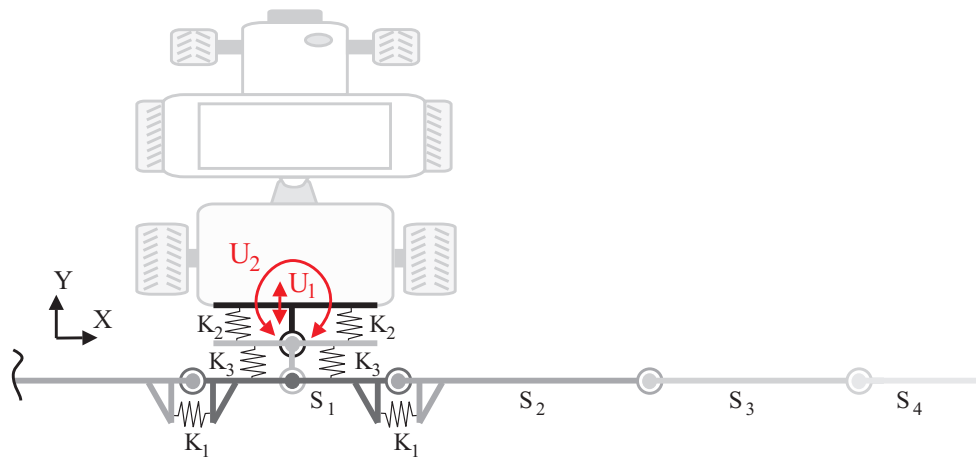


Figure 2: 2D-model of the sprayboom

cies and modeshapes as residues in the updating process, where parameter estimation is performed with sensitivity-based methods [4]. One of the advantages of this approach, is that modal parameters can be identified from output-only measurements, where the structure is excited by ambient loads. This way, the parameters can be estimated in operational conditions.

The number of parameters to be updated should be kept small in order to get a well-conditioned estimation problem. Therefore, a simplified model of the spray boom in combination with the trailer is proposed (figure 2). Besides, it is tested in different configurations to increase the number of updating equations. This technique is referred to as multi-model updating [5].

As the problem of model updating, also indirect identification of forces is classified in the category of inverse problems and thus suffers from ill conditioning. It becomes ill-posed when the number of potential input locations exceeds the number of modes, which can be problematic for the case forces are identified from experimental modal models [6, 7]. Here, forces are identified from an updated finite element model, so this should not be a problem. Since there are only two input locations, the problem should be well conditioned. For the identification of forces, the algorithm described by [8] is employed, which is implemented in FEMtools. This software is also used for updating the finite element model.

2 Spray boom model

The system under test is a John Deere 700 series prototype trailed sprayer (24m width, triple fold) in combination with a New Holland TS135 tractor. A simplified model of this system is proposed here.

The spray boom is modeled as a 2D structure in the horizontal plane (figure 2). Movements in the horizontal plane are most of our interest, because they have the largest effect on the spray distribution pattern. The large difference in stiffness of the spray boom in horizontal direction and vertical direction (figure 2) justifies the assumption of a 2D model. The boom is modeled by 2D beam elements whose mass properties are estimated from the manufacturer's data.

The dynamics of the tractor and trailer are not taken into consideration. Instead, the displacement of the trailer is used as input to the model. This implies that it has to be ensured that there is no interaction between the dynamics of the tractor-trailer combination and the spray boom. As inputs to the model, displacements of the trailer are selected rather than forces. This is achieved in FE-software by modeling the trailer as a point mass with very large inertia, making its motions insensitive to resonances of the beam. So, forces applied to this point mass are proportional to its acceleration amplitude. Displacements can be deduced from these accelerations. The two inputs of the system are translation in the y-direction U_1 , and rotation about the z-axis of the trailer U_2 .

Three different springs can be seen on figure 2. The first two (K_1 and K_2) are intended to improve the dynamic behavior of the spray boom, by lowering the eigenfrequencies. This way, damping can be increased by placing dampers at these locations. The third spring (K_3) represents the stiffness of bearings that are intended to guide the spray boom in the vertical direction.

The first two springs (K_1 and K_2) can be blocked, which allows to test the structure in three different configurations (table 1). The advantage is that more unknown parameters can be estimated, because the number of updating equations is increased. Besides, if identical forces are applied to the test system in the three configurations, the identified forces should be the same too. This way it can be checked whether the model is consistent.

To be sure that the forces applied to the system are the same in the three configurations, the model under test is first subjected to shaker excitations. Afterwards, field tests are performed to obtain the load spectrum in real field conditions.

configuration	K_1	K_2
1	blocked	blocked
2	K_1	blocked
3	blocked	K_2

Table 1: Configurations

3 Shaker experiments

3.1 Operational modal analysis

For the modal analysis experiment, the two wheels of the trailer are excited in vertical direction with two hydraulic shaker tables (figure 1). Double integrated white noise signals are applied to the position controllers of the shakers in the frequency band 0.2-10Hz.

Although excitation is performed with shakers, the input forces are not measured, because this experiment is meant as preparation for field measurements, where input forces cannot be measured. Therefore, modal parameters are estimated from output only data. A stochastic subspace method is applied for this purpose [9].

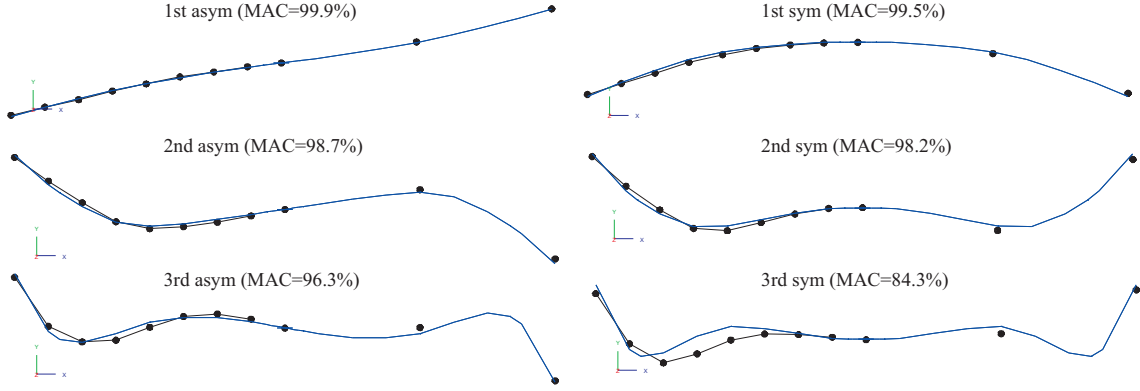


Figure 3: Modeshapes of updated finite element model (blue line) and modeshapes identified from operational modal analysis (dots); structure in configuration 1

Figure 4 shows the PSD of the accelerations measured at the beam tip for this experiment. Six eigenmodes are identified in the frequency range 0.2-10Hz. The modeshapes are plotted in figure 3. The location of the accelerometers is also shown in this figure. Eigenfrequencies and damping ratios are listed in table 2. A clear distinction between symmetrical and asymmetrical modes can be made.

3.2 model updating

The unknown parameters are estimated with a sensitivity-based method, that minimizes the difference between modal parameters identified from operational modal analysis and modal parameters obtained from finite element analysis. The updating parameters are the three spring stiffness's K_1 , K_2 and K_3 and the bending moments of inertia of the beam elements. It is assumed that the bending moments of inertia of the elements of the four sections S_1 , S_2 , S_3 and S_4 are identical for each section. So, 7 parameters have to be estimated. The residues are the 6 eigenfrequencies and 6 MAC-values.

Table 2 lists the percentage errors on the eigenfrequencies resulting from the updating process. In the case the three configurations are updated separately, the error is very small, with a mean absolute value of 0.2% for the first five frequencies. The error on the sixth eigenfrequency is noticeably higher (4.5%). This eigenfrequency is accounted for in the updating process with a lower weight, because assuming an equal weight increases the error on the other frequencies, which are considered as more important. The non-linear behavior of the hinge between the third and the fourth boomsection is responsible for this.

mode	Configuration 1				Configuration 2				Configuration 3			
	f_t (Hz)	ξ (%)	e_r (%)	$e_{r,m}$ (%)	f_t (Hz)	ξ (%)	e_r (%)	$e_{r,m}$ (%)	f_t (Hz)	ξ (%)	e_r (%)	$e_{r,m}$ (%)
1 st asym	0.68	1.73	0.10	-5.08	0.49	7.45	0.01	8.82	0.26	7.83	-0.01	-0.23
1 st sym	1.15	0.48	-0.36	0.44	0.76	6.94	-0.05	-2.09	1.15	0.59	-0.01	0.45
2 nd asym	3.01	4.57	-0.50	-2.94	2.86	3.30	-0.20	1.37	2.67	1.91	0.12	1.83
2 nd sym	4.00	0.81	0.84	0.40	3.33	3.34	0.18	-4.12	3.98	2.50	-0.20	0.94
3 rd asym	7.60	1.91	0.13	-0.14	7.52	4.83	0.18	0.75	7.35	1.28	0.34	0.95
3 rd sym	9.25	2.27	-5.04	-5.03	8.87	1.56	-3.05	-8.83	9.23	1.45	-5.55	-4.87

Table 2: Eigenfrequencies (f_t) and damping ratios (ξ) obtained from operational modal analysis and percentage error on the eigenfrequencies resulting from model updating of three configurations separately (e_r) and for the case of multi-model updating ($e_{r,m}$)

The percentage error on the eigenfrequencies for the case the three configurations are updated simultaneously is considerably higher, with a mean absolute value of 2% for the first five frequencies. Especially the error on the first eigenfrequency is large. The main difference between the three configurations is situated in the spring stiffness of the vertical bearings (K_2). This is not entirely unexpected considering the play in the bearings. For the multi-model updating case, the sixth eigenfrequency is not taken into account.

Notice the very good MAC values (figure 4), justifying the 2D representation of the 3D structure. Visible inspection and investigation of the vibration data also highlighted the presence of two torsional modes of the structure at 5Hz and 9.1Hz. However, their influence on the total response in the horizontal direction is low, so they are not taken into account.

3.3 Force identification

For the identification of forces, the algorithm described by Dascotte [8] is applied. This starts from the modal expansion of the dynamic flexibility matrix:

$$\{X\} = \sum_{i=1}^N \frac{\{\psi_i\}\{\psi_i\}^t}{\lambda_{r_i}^2 - \omega^2} \{F\} \quad (1)$$

where $\{F\}$ and $\{X\}$ are the vectors of harmonic forces applied to the structure and the resulting displacements, and ω , λ_{r_i} and $\{\psi_i\}$ are respectively the excitation frequency, the damped eigenfrequency and the corresponding modeshape. Inversion of equation (1) gives:

$$\{F\} = \sum_{i=1}^N \{\psi_i\}^+ \{\psi_i\}^t [M] \{X\} (\lambda_{r_i}^2 - \omega^2) \quad (2)$$

So, by calculating the pseudo-inverse of the modal matrix, a least squares approximation of the forces is obtained. Because the experimental responses usually don't cover all the degrees of freedom of the FE-model, the test data is expanded with the SEREP method. In case forces act on only $m < n$ degrees of freedom, $\{\psi\}^+$ can be reduced. This algorithm is implemented in FEMtools.

Now, if a time sample of the displacements is given, this signal should first be converted to frequency domain by taking the discrete fourier transform. Then, harmonic forces can be identified as described above and the time signal of the forces is obtained by taking the inverse discrete fourier transform.

Following this procedure, the time signals of the equivalent displacement inputs U_1 , and U_2 are identified from the measured spray boom accelerations. Modal damping is assumed here and damping ratios obtained from stochastic subspace identification of modal parameters are used for this purpose.

Figure 5 shows the PSD of these input displacements for the three configurations. Since the same signal is applied to the position controller of the shaker for the three experiments, the PSD's should be the same. However, there seems to be a significant difference in spectrum of the rotation input of configuration 3 compared to the other two spectra. It indicates an inconsistency between the model and the real structure, which could be caused by:

- Oversimplified model structure (2D)
- Simplification of the load path (only 2 input forces are considered)
- Interaction between dynamics of the trailer-tractor and sprayboom
- Nonlinear elements e.g. K_2 (cellasto springs) and K_3 (bearings with play)
- Assumption of modal damping, while the damping is clearly located in the spring elements

So, when simulations are performed, we should take into account that the response level can be underestimated by lowering the spring stiffness K_2 .

Locally, there are large differences between the PSD's caused by an error in eigenfrequency between the test model and the FE-model. This is certainly the case for lightly damped modes, such as the third symmetrical

mode. At 9Hz large peaks can be observed in the PSD of the translation input. In a lesser extend, this effect is also noticeable at the frequency of the first asymmetrical mode in the PSD of the rotation input (the model parameters obtained from multi-model updating are used here). The purpose is to estimate a parametric spectrum model from these PSD's, so this effect is not important. Frequency lines where such problems are encountered can be omitted in the estimation process.

Figure 4 shows the PSD of the spray boom response by applying the identified forces to the model. At the boom tip, there is an excellent agreement with the measured response. Though, the difference gets larger for responses at locations closer to the middle of the boom, which can be explained by the larger amplitudes of vibration at the beam tip having a stronger influence on the estimation process. Especially in the neighborhood of zero's there are large differences.

4 Field experiments

In this section, the previous procedure is applied to identify the load spectrum in field conditions. By driving on different fields with the sprayer, it is possible to make a classification of the obtained input displacement spectra, based on a parameterized spectrum model.

Damping properties can change with operational conditions. For foldable structures like spray booms, even eigenfrequencies can vary slightly from time to time. Therefore, for the field experiments, modal parameters should be re-estimated. Figure 7 shows the PSD of the boom tip accelerations driving with different speeds on a meadow. Aside from the eigenfrequencies of the spray boom, also speed dependent components are detected. This implies that identification of modal parameters is hampered, because these components are identified as well.

The existence of speed dependent components is explained by the correlation between the excitations under the different wheels. This implies that their mutual phase relationship is predetermined by the driving speed and the excitation frequency. When the rear wheels of the tractor are in anti-phase with the wheels of the trailer, horizontal excitation of the spray boom is larger than when they're in phase. This assumption is confirmed by figure 8. Here, the PSD of the identified loads is shown for different driving speeds. Vertical lines are drawn at the frequency lines where the rear wheels of the tractor and the wheel of the trailer are in phase. The front wheels of the tractor seem to have less influence in this.

Another consequence of the presence of speed dependent components is that the driving speed has a large effect on the boom movements. It is seen that for driving speeds of 6 km/h and 8.7 km/h the first symmetrical eigenfrequency corresponds to a speed dependent component, while driving at a speed of 7.3 km/h this is not the case (figure 7). The difference in amplitude of vibration is clear (factor 3).

The identified load spectrum for the three configurations can be found in figure 6. Note that the mutual difference is smaller compared to the tests on the shaker. The presence of a frequency component at 6.5Hz is explained by the tyre nibbles. In the PSD of the rotation input, the torsional mode at 9.1 Hz is also clearly visible.

Finally, figure 9 shows the load spectrum for three different fields: a field with maize stubbles and two meadows. In the second meadow tramlines are crossed, which gives a possible explanation for the lower excitation level. The identified time histories of the excitations can be used directly in simulations. However, because of the variable pattern caused by the speed dependent components, it seems more interesting to estimate a parametric model from the PSD's. This way a very rough classification is made between what is assumed to be representative for a normal spraying conditions and rough spraying conditions. A spectrum is assumed, of the form

$$S_{1,2}(\omega) = \frac{a_{1,2}}{\omega^{p_{1,2}}} \frac{1}{(1 + \omega/\omega_{c1,2})^{q_{1,2}}} \quad (3)$$

where ω is the frequency in rad/s and the indices $1,2$ refer to respectively the translation and rotation input. The coefficients are listed in table 3

field	a_1	ω_{c1}	p_1	q_1	a_2	ω_{c2}	p_2	q_2
normal	$9e-4$	7.5	1.5	4.5	$9e-5$	7.5	1	3.5
rough	$1.5e-4$	7.5	1.5	4.5	$1.5e-5$	7.5	1	3.5

Table 3: Coefficients of parametric spectrum model for normal and rough spraying conditions

Assuming that the excitations are stationary random processes with a Gaussian distribution and zero mean value, the statistical description of the excitations is completely determined by the spectrum. Time records can be generated by an inverse Fourier transform:

$$u_{1,2}(t) = \sum_{i=1}^N \sqrt{2S_{1,2}(\omega_i)\Delta\omega} \cos(\omega_i t + \theta_i) \quad (4)$$

where θ_i is the random phase with a uniform distribution in the interval from 0 to 2π .

Because the coherence of the two inputs is low (figure 10) they can be treated as independent inputs.

5 Conclusion

A simple 2D finite element model of a spray boom is proposed, that represents its dynamic behavior. The parameters of the model are updated with experimental output-only vibration data and input forces are identified from these data. The model is tested in three configurations to improve the condition of the updating process.

By applying the same forces to the model in three configurations, the identified forces should be the same to ensure a consistent model. This is checked first by shaker experiments, because this way it can be ensured that the applied forces are the same. A clear difference is noticeable in the identified force spectrum of one of the configurations compared to the other two. However, this distinction is less pronounced in the field experiments. By a lack of data it is not possible to draw concrete conclusions from this. The obtained model is considered as a good simplified linear approximation of the dynamic behavior of the complex structure, but we should keep in mind that the response level can be underestimated by lowering the spring stiffness K_2 when simulations are performed with this model.

Speed dependent frequency components seem to influence the identification process when field experiments are performed. It is shown that they are caused by the correlation of the excitations to the tires. Their presence allows only to make a very rough classification of different excitation spectra.

6 Acknowledgements

The authors want to express their gratitude to the FWO Vlaanderen (Fund of Scientific Research Flanders) for their financial support: OMAX project G.0343.04 and Jan Anthonis is financed by the FWO as post-doctoral fellow.

This research was also funded by the Interuniversity Attraction Poles program - Belgian Science Policy

References

- [1] C.J. Dodds, J.D. Robson, *The description of road surface roughness*, Journal of Sound and Vibration, Vol. 32, No. 2, (1973), pp. 175-183.

- [2] D. Ooms, R. Ruter, F. Lebeau, M.-F. Destain *Impact of the horizontal movements of a sprayer boom on the longitudinal spray distribution in field conditions*, Crop Protection, Vol. 22, (2003), pp. 813820.
- [3] J.E. Mottershead, M.I. Friswell *Model updating in structural dynamics: a survey*, Journal of Sound and Vibration, Vol. 167, No. 2, (1993), pp. 347-375.
- [4] A. Teughels, *Inverse modelling of civil engineering structures based on operational modal data*, Phd. thesis, Katholieke Universiteit Leuven, Departement Burgerlijke Bouwkunde, Leuven (2003).
- [5] T. Lauwagie, H. Sol, W. Heylen, G. Roebben, *Determination of the in-plane elasticproperties of the different layers of laminated plates by means of vibration testing and model updating*, Journal of Sound and Vibration, Vol. 274, (2004), pp. 529546.
- [6] M. Corus, E. Balms, *A priori verification of local FE model based force identification*, Proceedings of ISMA 2004 International Conference on Noise and Vibration Engineering, Leuven, Belgium, 20-22 September (2004).
- [7] E. Parloo, P. Verboven, P. Guillaume, M. Van Overmeire, *Force identification by means of in-operation modal models*, Journal of Sound and Vibration, Vol. 262, (2003), pp. 161173.
- [8] E. Dascotte, J. Strobbe, *Identification of pressur forces in a cavity using an inverse solution method*, Proceedings of ISMA 1998 International Conference on Noise and Vibration Engineering, Leuven, Belgium, 16-18 September (1998).
- [9] B. Peeters, G. De Roeck, *Reference based stochastic subspace identification in civil engineering*, Inverse Problems in Engineering, Vol. 8, No. 1, (2000), pp. 4774.

7 Graphs

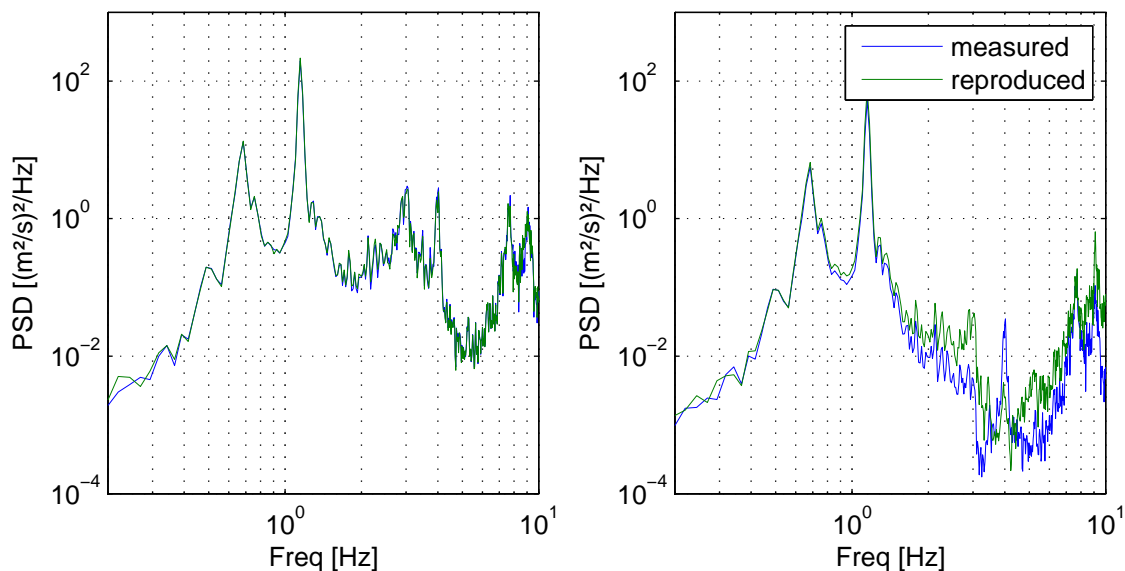


Figure 4: PSD of measured spray boom accelerations (excitation by shaker and structure in configuration 1) and the accelerations obtained by applying the identified forces to the finite element model: at boom tip (left) and 3m from the boom tip (right)

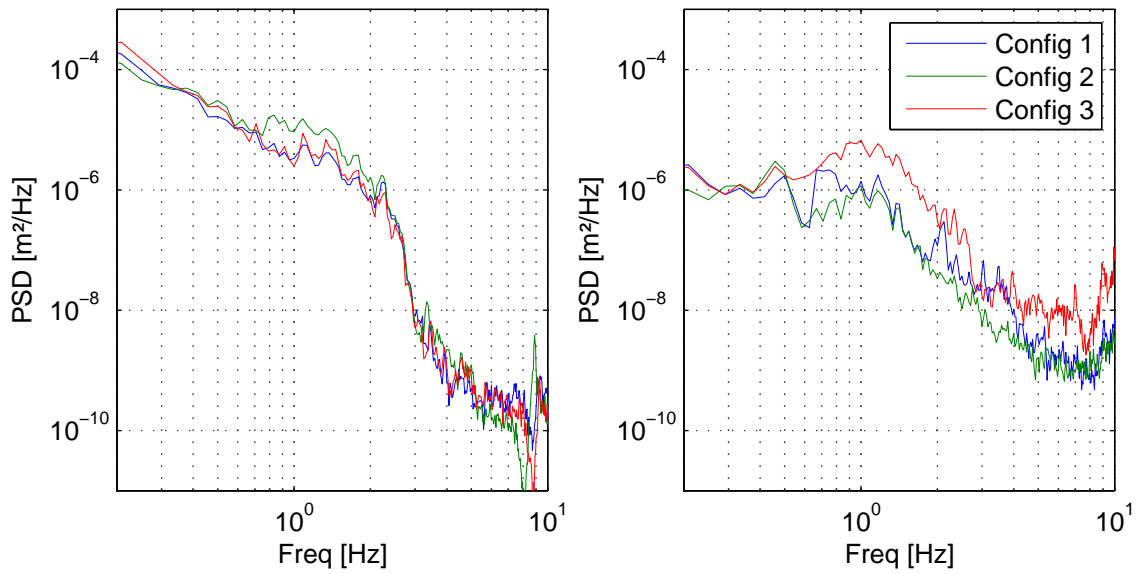


Figure 5: PSD of identified input excitations for 3 different configurations (excitation by shaker): translation input U_1 (left) and rotation input U_2 (right)

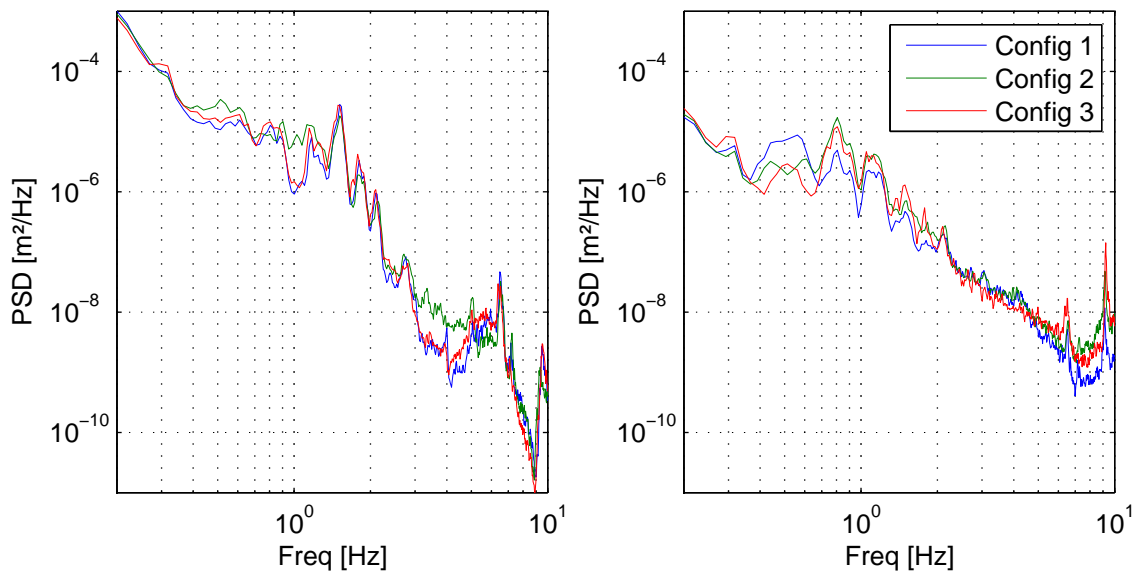


Figure 6: PSD of identified input excitations for 3 different configurations, driving on meadow 2 : translation input U_1 (left) and rotation input U_2 (right)

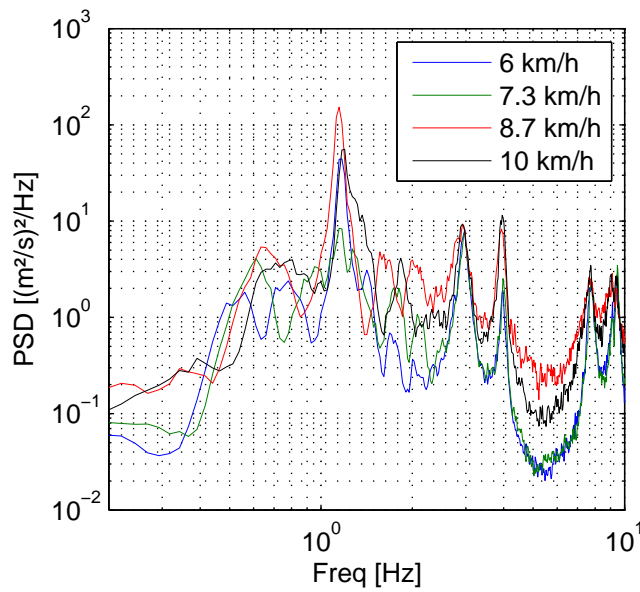


Figure 7: PSD of measured spray boom accelerations driving on meadow 2 for different driving speeds (structure in configuration 1)

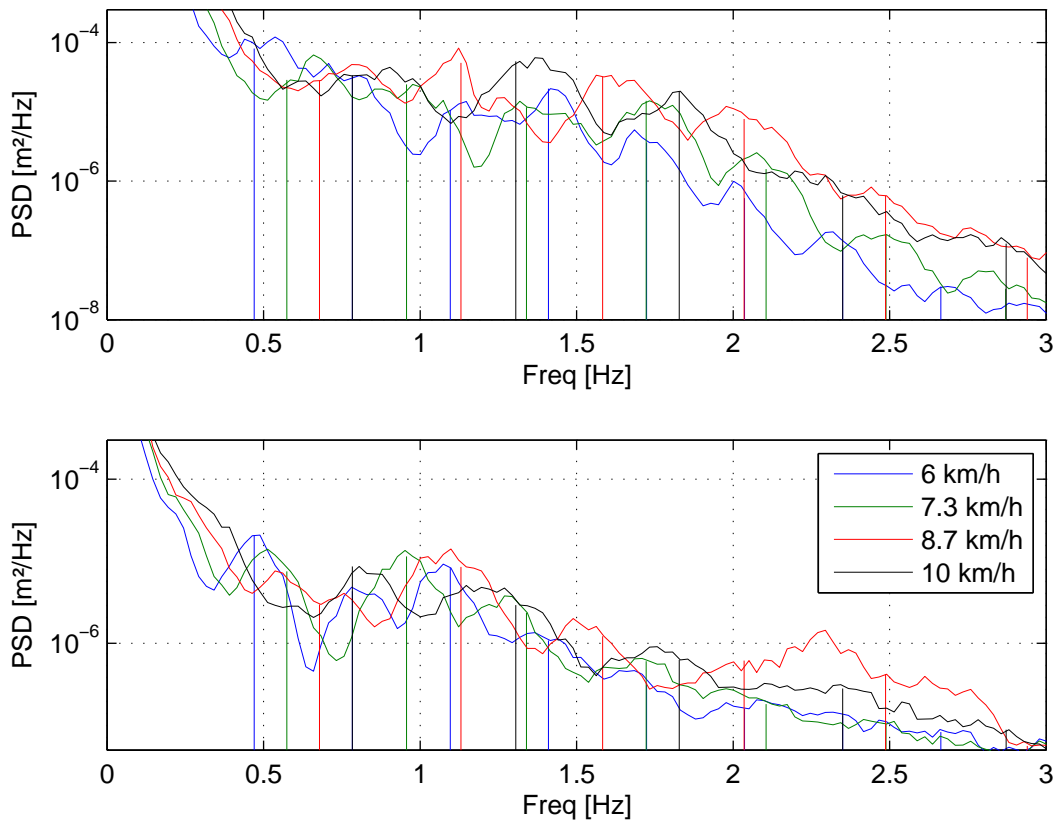


Figure 8: PSD of identified input excitations for different driving speeds, driving on meadow : translation input U_1 (top) and rotation input U_2 (bottom); vertical lines coincide with frequencies where rear wheel of tractor is in phase with wheel of trailer (structure in configuration 1)

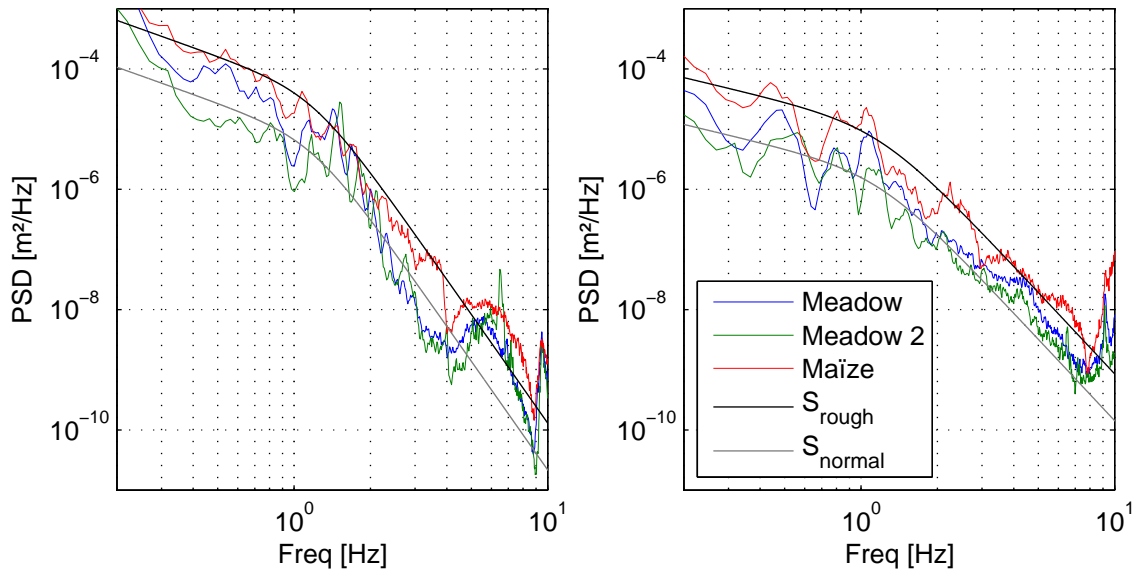


Figure 9: PSD of identified input excitations driving on different fields and estimated parametric spectrum; (structure in configuration 1); translation input U_1 (left) and rotation input U_2 (right)

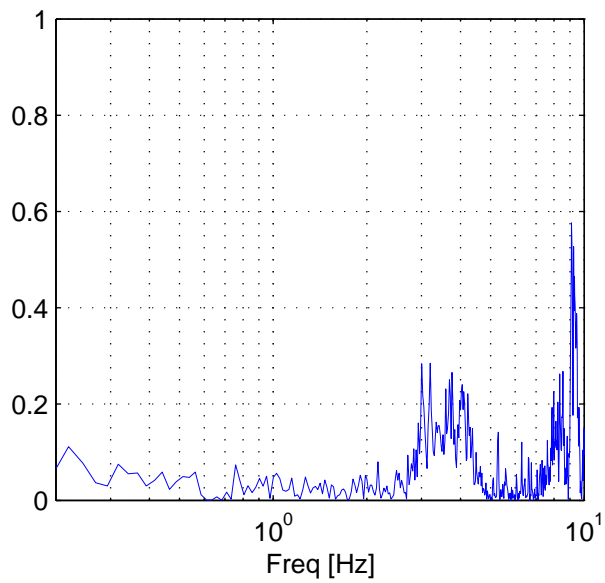


Figure 10: Coherence of translation excitation U_1 and rotation excitation U_2